



TCAD-Based Extraction of Breakdown Voltage in pGaN HEMTs

Anirudh Mittal Priyesh Kumar Jhuma Saha

Indian Institute of Technology Gandhinagar



Abstract

This work presents a TCAD-based study of breakdown voltage in p-GaN gate HEMTs. A literature-based structure was simulated in Synopsys Sentaurus with variations in material and structural parameters. Breakdown voltages were extracted via transient drain sweeps. The results highlight the influence of design choices on high-voltage performance.

Introduction

Gallium Nitride based High Electron Mobility Transistors (HEMTs) have emerged as a leading solution for next-generation power electronics due to their intrinsic normally-off operation, high breakdown strength, and robust gate control. Their use of wide bandgap GaN layers ensures strong field-handling capability and excellent thermal stability—making them well-suited for high-voltage and high-frequency applications in compact systems.

This study investigates the breakdown voltage behavior of p-GaN HEMTs through detailed TCAD simulations by varying buffer configuration, substrate material, doping, and layer parameters. The findings establish key design strategies for optimizing device reliability under extreme electric fields.

TCAD Structure of pGaN HEMT

The simulated device is a lateral p-GaN gate HEMT based on a literature-referenced III-nitride stack. Ohmic source and drain contacts are formed via recess etching, while the gate employs a Schottky contact with a tungsten metal electrode. The structure was constructed using Sentaurus SDE with mesh refinement at critical field regions.

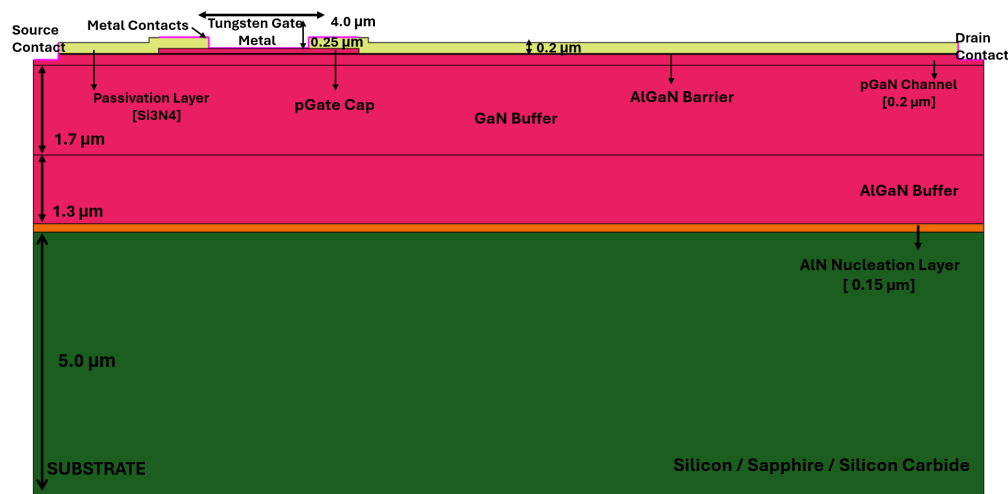


Figure 1. Simulated cross-section of the p-GaN gate HEMT structure.

Simulations in SDevice incorporate drift-diffusion transport, polarization and tunneling effects, trap dynamics, and impact ionization. Breakdown voltage was extracted via transient drain bias sweeps, with structural parameters varied to evaluate their impact on critical field behavior.

Parameter	Value
Carbon Doping Density in Buffer Layers	$1 \times 10^{19} \text{ cm}^{-3}$
p-GaN Gate Layer Thickness	$0.1 \mu\text{m}$
Gate Metal Length	$4.0 \mu\text{m}$
Gate Contact Length	$2.0 \mu\text{m}$
Gate Source Spacing	$2.0 \mu\text{m}$
Gate Drain Spacing	$12.0 \mu\text{m}$
p-GaN Region Length	$4.0 \mu\text{m}$

Table 1. Key geometric and doping parameters used in the TCAD simulation.

Variation of Model Parameters

Two buffer configurations were simulated to assess their impact on breakdown behavior. The first used an AlGaN buffer beneath a GaN channel; the second employed a full GaN buffer. The GaN-only structure exhibited superior breakdown performance.

Table 2. Breakdown voltage under different buffer and substrate conditions

Buffer	Substrate	x_B	t_B (μm)	N_{Mg} (cm^{-3})	V_{br} (V)
AlGaN	Silicon	0.25	0.02	1.50×10^{19}	421.88
	SiC_4H	0.25	0.02	1.50×10^{19}	408.22
GaN	Silicon	0.3	0.013	2.00×10^{19}	728.92
	SiC_4H	0.3	0.013	1.50×10^{19}	1119.25

This configuration was adopted for all subsequent parameter variations. Key parameters were then varied: substrate material, barrier mole fraction (x_B), barrier thickness (t_B), and magnesium doping concentration (N_{Mg}). Each variation's effect on breakdown voltage and electric field was evaluated.

References

- [1] X.-G. He, D.-G. Zhao, and D.-S. Jiang, "Formation of two-dimensional electron gas at algan/gan heterostructure and the derivation of its sheet density expression," *Chinese Physics B*, vol. 24, no. 6, p. 067301, 2015.
- [2] I. Hwang, M. Kim, S. Baik, H. Kim, K. Lee, T. Kim, and S. Ryu, "p-gan gate hemts with tungsten gate metal for high threshold voltage and low gate current," *IEEE Electron Device Letters*, vol. 34, no. 2, pp. 202–204, 2013.
- [3] Y. Wang, S. Hu, J. Guo, H. Wu, T. Liu, and J. Jiang, "Enhancement of breakdown voltage in p-gan gate algan/gan hemts with a stepped hybrid gan/aln buffer layer," *IEEE Journal of the Electron Devices Society*, vol. 10, pp. 197–202, 2022.

Results and Observations

The resulting breakdown voltage (V_{br}) and peak electric field (E_{max}) for each configuration were simulated and are summarized below.

Substrate	x_B	t_B (μm)	N_{Mg} (cm^{-3})	V_{br} (V)	E_{max} (V/cm)
Al_2O_3	0.25	0.02	1.50×10^{19}	49.10	3.38×10^6
	0.25	0.02	2.00×10^{19}	54.53	4.12×10^6
	0.25	0.013	1.50×10^{19}	996.83	8.81×10^6
	0.25	0.013	2.00×10^{19}	1010.25	8.93×10^6
	0.25	0.015	1.50×10^{19}	986.44	4.83×10^6
	0.25	0.015	2.00×10^{19}	1012.58	5.81×10^6
	0.3	0.02	1.50×10^{19}	14.87	3.52×10^6
	0.3	0.02	2.00×10^{19}	18.11	3.63×10^6
	0.3	0.013	2.00×10^{19}	378.86	3.44×10^6
	0.3	0.013	1.50×10^{19}	777.74	3.56×10^6
	0.3	0.01	2.00×10^{19}	808.31	5.67×10^6
	0.3	0.01	2.00×10^{19}	1119.25	8.12 $\times 10^6$
4H-SiC	0.25	0.02	1.50×10^{19}	69.18	3.17×10^6
	0.25	0.02	2.00×10^{19}	111.96	3.20×10^6
	0.25	0.013	1.50×10^{19}	882.01	4.29×10^6
	0.25	0.013	2.00×10^{19}	889.91	4.29×10^6
	0.25	0.013	1.50×10^{19}	886.17	4.38×10^6
	0.25	0.015	2.00×10^{19}	901.40	4.29×10^6
	0.3	0.02	1.50×10^{19}	14.91	3.51×10^6
	0.3	0.02	2.00×10^{19}	18.15	3.53×10^6
	0.3	0.013	1.50×10^{19}	135.47	4.42×10^6
	0.3	0.013	2.00×10^{19}	1091.72	4.41×10^6
	0.3	0.013	1.50×10^{19}	1119.25	8.12 $\times 10^6$
	0.3	0.01	2.00×10^{19}	1118.23	8.01×10^6
Silicon	0.25	0.02	1.50×10^{19}	103.62	3.11×10^6
	0.25	0.02	2.00×10^{19}	627.37	3.79×10^6
	0.25	0.013	1.50×10^{19}	630.65	4.41×10^6
	0.25	0.013	2.00×10^{19}	631.03	4.53×10^6
	0.25	0.015	1.50×10^{19}	639.14	4.55×10^6
	0.25	0.015	2.00×10^{19}	639.53	4.31×10^6
	0.3	0.02	1.50×10^{19}	14.93	3.59×10^6
	0.3	0.02	2.00×10^{19}	310.49	4.16×10^6
	0.3	0.013	2.00×10^{19}	728.92	4.14×10^6
	0.3	0.013	1.50×10^{19}	715.37	4.12×10^6
	0.3	0.01	2.00×10^{19}	715.37	4.55×10^6
	0.3	0.01	2.00×10^{19}	1119.25	8.12 $\times 10^6$

Table 3. Breakdown voltage and peak electric field across substrates for varying x_B , t_B , and Mg doping.

We further analyzed the electric field distribution of configuration that yielded the highest breakdown voltage: **1119.25 V** observed on the **4H-SiC** substrate with $x_B = 0.3$, $t_B = 0.013 \mu\text{m}$, and $N_{Mg} = 1.50 \times 10^{19} \text{ cm}^{-3}$ to get insight into breakdown behavior.

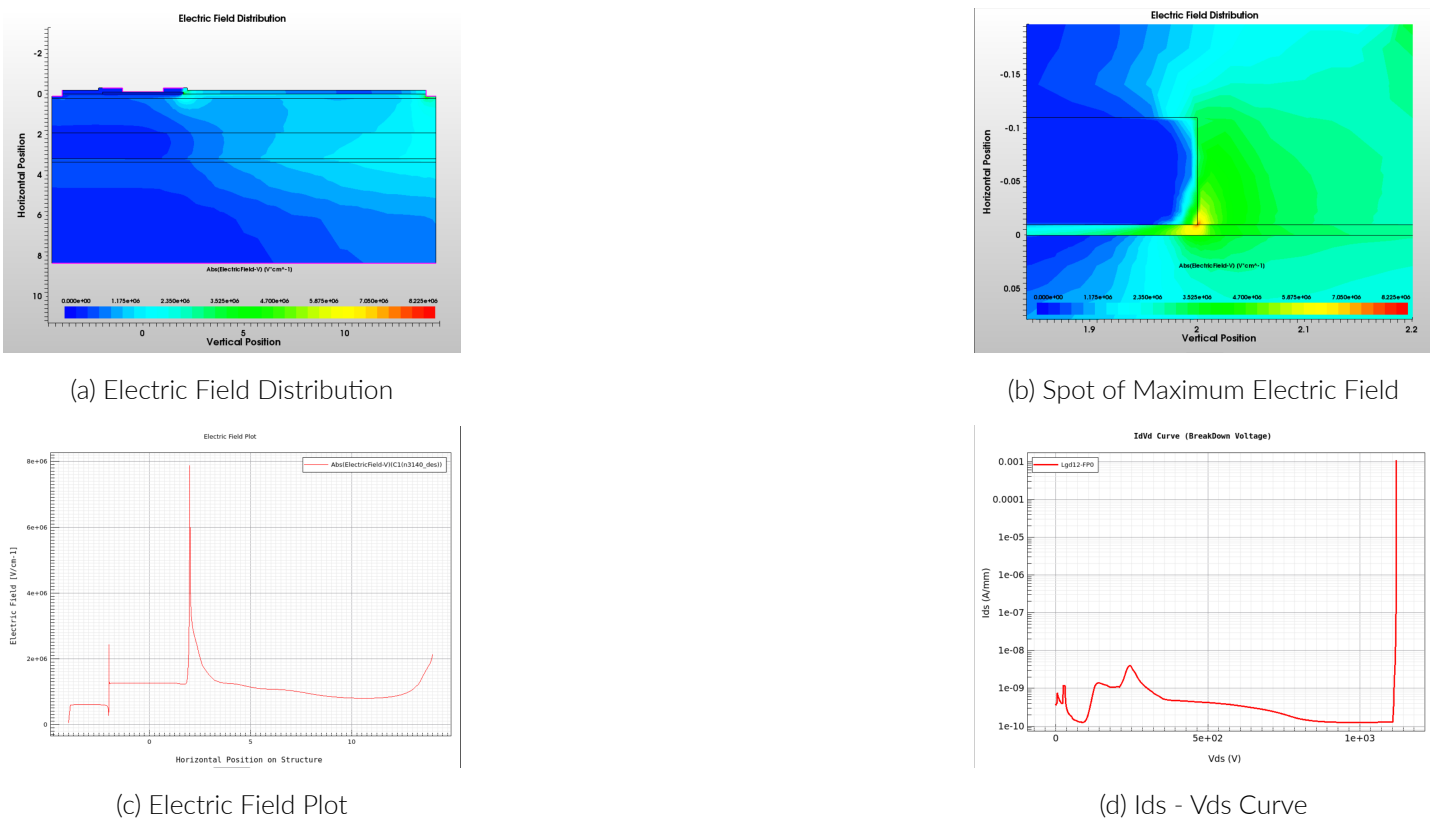


Figure 2. Electric Field and Breakdown Analysis

Conclusion

The breakdown voltage was found to improve with a decrease in Al mole fraction (x_B) and barrier thickness (t_B) across all substrates, minimizing interface fields and enhancing depletion. Lower Mg doping ($1.5 \times 10^{19} \text{ cm}^{-3}$) yielded better performance on 4H-SiC and Al_2O_3 , likely due to reduced ionized impurity scattering. In contrast, higher doping slightly benefited Silicon due to enhanced channel control. Among all configurations, the 4H-SiC-based structure exhibited the best breakdown behavior, reaching 1119.25 V and $8.12 \times 10^6 \text{ V/cm}$ under optimal conditions.

Future Work

Future work can explore heterostructure modifications such as the Stepped GaN/AlN hybrid buffer, which demonstrated a 67.8 % increase in breakdown voltage. This approach enables better field modulation and is promising for next-generation high-power HEMTs.

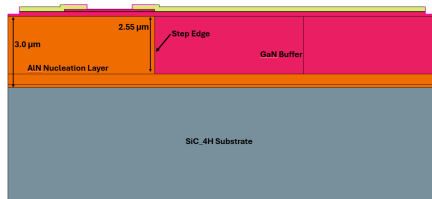


Figure 3. Stepped GaN/AlN hybrid buffer for enhancing breakdown performance.

Acknowledgement

This work was carried out under the supervision of Prof. Jhuma Saha at the NanoDC Laboratory, IIT Gandhinagar. The author gratefully acknowledges her guidance and support throughout the project.